Electrochemical and Solid-State Letters, **12** (8) H309-H311 (2009)
1099-0062/2009/12(8)/H309/3/$25.00 © The Electrochemical Society

Room-Temperature Indium-Free Ga:ZnO/Ag/Ga:ZnO Multilayer Electrode for Organic Solar Cell Applications

Ho-Kyun Park,[a] Jin-A Jeong,[a] Yong-Seok Park,[a] Seok-In Na,[b] Dong-Yu Kim,[b] and Han-Ki Kim[a,z]

[a]*Department of Display Materials Engineering, Kyung Hee University, Gyeonggi 446-701, South Korea*
[b]*Heeger Center for Advanced Materials, Department of Materials Science and Engineering, Gwangju Institute of Science and Technology, Gwangju 500-712, South Korea*

We reported on the characteristics of an indium-free Ga-doped ZnO (GZO)/Ag/GZO multilayer electrode for use in bulk heterojunction organic solar cells. By inserting a very thin Ag layer between two GZO layers, we can fabricate a GZO-based transparent electrode with a low sheet resistance of 6 Ω/□ and a high optical transmittance of 87% at room temperature without postannealing. The power conversion efficiency (2.84%) of the organic solar cell fabricated on the GZO/Ag/GZO multilayer using neutral poly(3,4-ethylenedioxythiophene):poly(styrenesulfonate) (PEDOT:PSS) is much higher than that of the organic solar cell fabricated on the GZO electrode (1.57%) annealed at 500°C. Indium-free GZO/Ag/GZO multilayer electrodes are expected to substitute for expensive indium tin oxide (ITO) electrode and decrease the cost of organic solar cells or flexible organic solar cells due to their comparable electrical and optical properties to those of crystalline ITO electrodes.
© 2009 The Electrochemical Society. [DOI: 10.1149/1.3149537] All rights reserved.

Manuscript submitted April 3, 2009; revised manuscript received May 14, 2009. Published June 8, 2009.

Bulk heterojunction organic solar cells (OSCs) have recently attracted considerable interest for use in the next generation of renewable energy sources due to their simple cell structure, simple process, low cost, and possibility of continuous roll-to-roll process in the atmosphere.[1,2] A key merit of OSCs is their potential for low cost and large area production based on continuous roll-to-roll coating.[3] Therefore, it is necessary to develop low cost transparent anode materials, which can be prepared at the lowest possible temperature, to enable the low cost production of OSCs. However, most OSCs reported so far are usually fabricated on dc or radio-frequency sputtered crystalline indium tin oxide (ITO) electrodes prepared at a temperature above 300°C. Considering the cost advantages of OSCs, ITO electrodes are not suitable due to the high cost of indium (the main component of ITO) and its limited availability. For these reasons, indium-free transparent conducting oxide (TCO), single-walled carbon nanotube films, and organic electrodes have been explored as potential low cost anode materials.[4-6] Recently, Ga-doped ZnO (GZO) electrodes have been employed as inexpensive anode materials for organic light-emitting diodes (OLEDs) and OSCs.[7-9] Bhosle et al. reported that small molecule-based OSCs fabricated on crystalline GZO electrodes showed a power conversion efficiency (PCE) of 1.25% which is comparable to that of ITO-based small molecule OSCs.[8] Owen et al. reported that the PCE of polymer solar cells fabricated on a crystalline GZO anode sputtered at 500°C is 0.35%, due to the small work function of the GZO electrode (4.23 eV).[9] However, there have been no reports on the fabrication of OSCs on amorphous GZO electrodes sputtered at room temperature, which would be beneficial for the low cost production of OSCs.

In this article, we report the characteristics of an indium-free GZO/Ag/GZO multilayer electrode grown by dual-target dc sputtering at room temperature. Using the metallic resistivity and antireflection effect of the Ag layer inserted between the GZO layers with optimized thickness, we can obtain a low sheet resistance of 6 Ω/□ and a high optical transmission of 87% matching the absorption region of the organic active layer. We fabricated an OSC on the GZO/Ag/GZO electrode with a higher PCE than that of the OSCs fabricated on the GZO electrode annealed at 500°C using a neutral poly(3,4-ethylenedioxythiophene):poly(styrenesulfonate) (PEDOT:PSS) solution.

Both top and bottom GZO electrodes, 40 nm thick, were deposited on a glass substrate by tilted dual-target dc magnetron sputtering at room temperature. At a constant dc power of 100 W, an Ar flow rate of 15 sccm, and a working pressure of 3 mTorr, a 40 nm thick bottom GZO layer was sputtered with a 3 in. GZO target (3 wt % Ga_2O_3-doped ZnO) at room temperature without substrate heating. After the sputtering of the bottom GZO layer, Ag layers with various thicknesses were sputtered on the bottom GZO layer at a constant dc power of 20 W, an Ar flow rate of 15 sccm, and a working pressure of 3 mTorr using a metallic Ag target. Subsequently, a 40 nm thick top GZO layer was deposited on the thin Ag layer under identical conditions to those used for the bottom GZO layer. For comparison, we prepared the as-grown and GZO electrodes annealed at 500°C with 500 nm thicknesses. Bulk heterojunction OSCs were prepared on both GZO/Ag/GZO and single GZO electrodes. After conventional electrode cleaning, the widely used PEDOT:PSS (CLEVIOS P VP AI 4083, H. C. Starck) and neutral PEDOT:PSS (Orgacon neutral pH, Agfa Gevaert NV) were spin coated on the GZO/Ag/GZO and ~20 nmthick single GZO electrodes, followed by drying at 120°C for 10 min in air using a hot plate. A blend solution of 25 mg of poly(3-hexylthiophere) (P3HT, Rieke Metals) and 25 mg of 1-(3-methoxycarbonyl)-propyl-1-phenyl-(6,6) C61 (PCBM, Nano-C) in 1 mL of 1,2-dichlorobenzene was spin coated on top of the respective PEDOT:PSS layers in a N_2 atmosphere. Then, a solvent-annealing treatment was performed by keeping the active films inside a covered glass jar for 2 h directly after spin coating, followed by additional thermal annealing at 110°C for 10 min, forming the ~230 nm thick active layer. Finally, Ca(20 nm)/Al(100 nm) layers were deposited on the P3HT:PCBM active layer as a cathode using a thermal evaporator system with a metal shadow mask. The photocurrent density–voltage (J-V) curves were measured using a Keithley 4200 source measurement unit in a N_2-filled glove box.

Table I compares the sheet resistance, resistivity, and transmittance of the as-grown GZO, GZO annealed at 500°C, and GZO/Ag/GZO electrodes. The as-grown GZO electrode shows a high sheet resistance of 1012 Ω/□ and a resistivity of 1.4×10^{-2} Ω cm.

Table I. Comparison of electrical and optical properties of as-grown GZO (amorphous), GZO annealed at 500°C (crystalline), and GZO/Ag/GZO (amorphous) multilayer electrodes prepared at room temperature.

	Sheet resistance (Ω/□)	Resistivity (Ω cm)	Transmittance at 550 nm (%)
As-grown GZO	1012	5.1×10^{-2}	78.1
GZO annealed at 500°C	24	1.4×10^{-3}	94.5
GZO/Ag (12 nm)/GZO	6	5.53×10^{-5}	87.2

[z] E-mail: imdlhkkim@khu.ac.kr

Downloaded 25 Apr 2010 to 159.226.100.225. Redistribution subject to ECS license or copyright; see http://www.ecsdl.org/terms_use.jsp

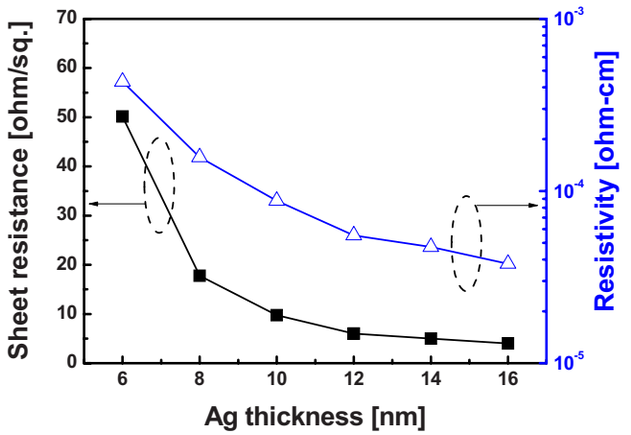

Figure 1. (Color online) The sheet resistance and resistivity of a GZO(40 nm)/Ag/GZO(40 nm) multilayer as a function of Ag thickness, which was continuously sputtered at room temperature.

However, the resistivity of the GZO film that was rapidly thermal annealed at 500°C decreased by 1 order of magnitude due to the increase in the carrier concentration caused by the substitution of Ga^{3+} ions into the Zn sites in the ZnO lattice.[10] The optical transmittance of the GZO film annealed at 500°C (94.5%) is much higher than that of the as-grown GZO film (78.1%). The optimized GZO/Ag/GZO electrode showed a very low resistivity and high transmittance, even though it was prepared at room temperature without an additional annealing process. The dependence of the electrical and optical properties on the Ag thickness is shown in Fig. 1. Although the as-grown GZO electrode showed a fairly high sheet resistance and resistivity at room temperature, the insertion of the Ag layer resulted in a significant reduction in the sheet resistance and resistivity. Above a 12 nm Ag thickness, the GZO/Ag/GZO electrode shows a very low sheet resistance (5–6 Ω/□) and resistivity ($\sim 10^{-5}$ Ω cm), which are both much lower than those of the crystalline ITO electrode.

Figure 2a shows the variation of the optical transmittance of the GZO/Ag/GZO electrode with Ag thickness. The optical transmittance of the GZO/Ag/GZO electrode at a wavelength of 400–600 nm increased remarkably with increasing Ag thickness. This could be attributed to the Ag layer reflecting light in the IR range and the

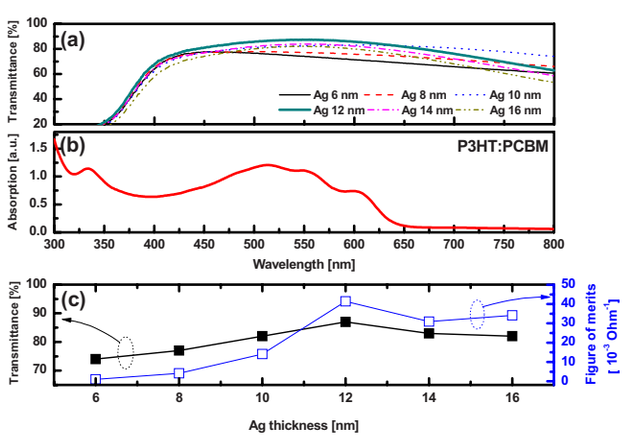

Figure 2. (Color online) (a) Optical transmittance of GZO/Ag/GZO electrode as a function of Ag thickness. (b) Absorption wavelength region of P3HT:PCBM active layer. (c) Figure of merit value of GZO/Ag/GZO electrode calculated from sheet resistance (R_{sh}) and optical transmittance (T) at a wavelength of 550 nm as a function of Ag thickness.

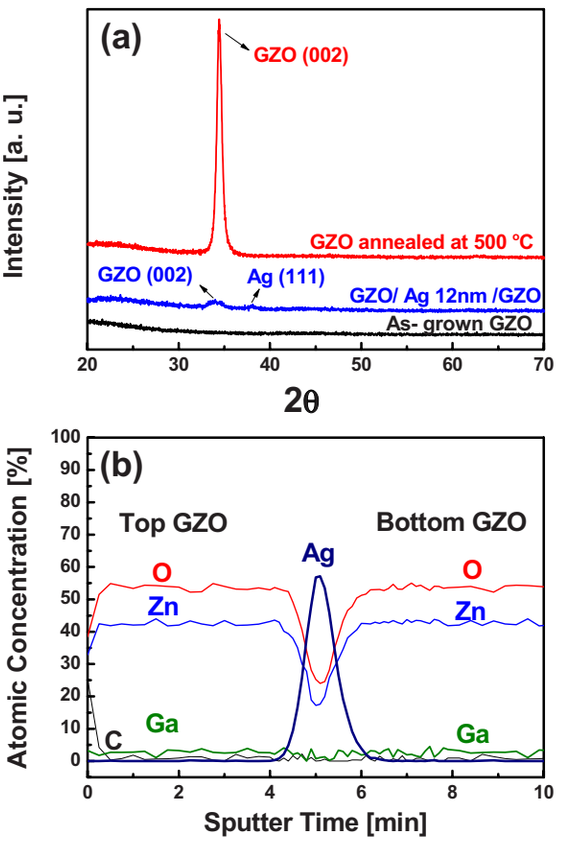

Figure 3. (Color online) (a) X-ray diffraction plots of GZO annealed at 500°C, as-grown GZO, and optimized GZO/Ag (12 nm)/GZO multilayer electrode. (b) AES depth profile of optimized GZO/Ag(12 nm)/GZO electrode showing the stable interface between Ag and GZO layers.

GZO suppressing the reflection from a Ag layer in the visible range.[11] At a 12 nm Ag thickness, the highest transmittance of 87.2% at a wavelength of 550 nm was observed. However, further increasing the Ag thickness above 12 nm resulted in a decrease in the transmittance, especially in the high wavelength region above 600 nm. Considering the absorption wavelength of the organic active layer (P3HT:PCBM) in Fig. 2b, it was thought that the low optical transmittance of the GZO/Ag/GZO electrode in the high wavelength region would not affect the performance of the OSCs. To determine the optimized Ag thickness in the GZO/Ag/GZO electrode, we calculated the figure of merit value ($\phi_{TC} = T^{10}/R_{sh}$) using the transmittance (T) at a wavelength of 550 nm and sheet resistance (R_{sh}), as shown in Fig. 2c.[12] The maximum ϕ_{TC} value (41.4 $\times 10^{-3}$ Ω^{-1}) of the GZO/Ag/GZO electrode was obtained at a 12 nm Ag thickness ($T = 0.87\%$ and $R_{sh} = 6$ Ω/□).

Figure 3a shows the X-ray diffraction plots obtained from the as-grown GZO, GZO annealed at 500°C, and GZO/Ag/GZO electrodes. The optimized GZO/Ag/GZO electrode shows broad peaks at ~34.02 and ~38.10°, corresponding to the amorphous GZO and Ag layer, respectively, due to the room-temperature sputtering process. However, the GZO film annealed at 500°C shows a strong (002) peak at 34.44° indicating that the annealed GZO films are textured with the c axis perpendicular to the glass substrate. In general, it is difficult to use an as-grown GZO film with an amorphous structure as an electrode in OLEDs organic photovoltaics (OPVs), due to the high resistivity of the inactivated GZO film. However, the GZO/Ag/GZO electrode could be directly employed in OPVs or flexible OPVs without a postannealing process, even though the top and bottom GZO layers have an amorphous structure. Figure 3b shows

Downloaded 25 Apr 2010 to 159.226.100.225. Redistribution subject to ECS license or copyright; see http://www.ecsdl.org/terms_use.jsp

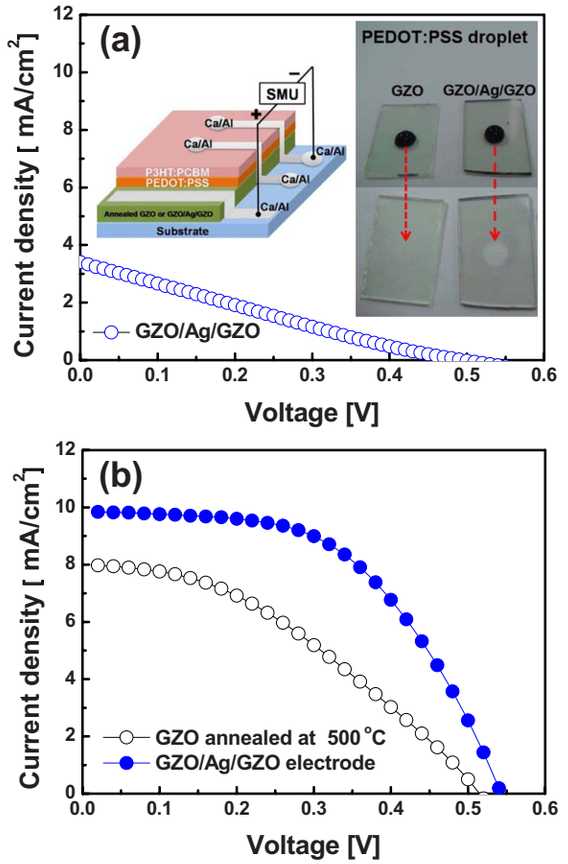

Figure 4. (Color online) (a) Current density (J)–voltage (V) characteristics of bulk heterojunction OSCs fabricated on a GZO/Ag/GZO multilayer electrode using conventional PEDOT:PSS with the inset showing the schematic OSC structure and picture of the etching of the GZO electrode by the PEDOT:PSS droplet. (b) Comparison of J-V characteristics of OSCs fabricated on a GZO/Ag/GZO electrode and annealed GZO single layer using neutral PEDOT:PSS.

the Auger electron spectroscopy (AES) depth profile of the optimized GZO/Ag/GZO electrode. It was shown that the individual bottom GZO, Ag, and top GZO layers were well defined without any interfacial layers due to the continuous sputtering process at room temperature. There is no evidence of an interfacial reaction between the Ag and GZO layers due to the stability of the GZO layer at room temperature. Considering the formation enthalpy of ZnO (−350.4 kJ/mol) and Ga_2O_3 (−1089.1 kJ/mol), the dissociation of GZO by the formation of a Ag_2O (−31.1 kJ/mol) layer cannot easily occur at room temperature.[13]

Figure 4 shows the photocurrent density–voltage (J-V) curves obtained under 100 mW/cm^2 illumination with an air mass (AM) 1.5 G condition of the OSCs fabricated on the annealed GZO and GZO/Ag/GZO electrodes. The OSCs fabricated on the GZO/Ag/GZO electrode using a conventional PEDOT:PSS layer (VP AI 4083) showed very poor performance with a fill factor (FF) of 0.23 and a PCE of 0.38% due to the severe reaction between GZO and conventional PEDOT:PSS. The J-V characteristics of the OSCs fabricated on the GZO electrode annealed at 500°C could not be measured due to the complete etching of the single GZO layer by PEDOT:PSS. The inset of Fig. 4a shows that the droplet of conventional PEDOT:PSS on the single GZO or GZO/Ag/GZO electrodes led to the removal of the GZO layer. Because the ZnO film was easily etched in the acidic solution, the PEDOT:PSS with pH in the range of 1–2 could remove the GZO electrode.[1] Thus, we exchanged the PEDOT:PSS solution with a neutral PEDOT:PSS solution to avoid the wet etching of the GZO electrode. Figure 4b shows the J-V curve of the OSC fabricated on the annealed GZO and GZO/Ag/GZO electrodes using a neutral PEDOT:PSS solution. The OSCs fabricated on the GZO/Ag/GZO electrode grown on glass showed an open-circuit voltage (V_{OC}) of 0.54 V, a short-circuit current (J_{SC}) of 9.86 mA cm^{-2}, an FF of 0.53, and a calculated PCE of $\eta_{AM\ 1.5}$ = 2.84%. However, the OSC fabricated on the annealed GZO layer showed a V_{OC} of 0.52 V, a J_{SC} of 8.00 mA cm^{-2}, an FF of 0.39, and a PCE of $\eta_{AM\ 1.5}$ = 1.57%. Until now, there have been no reports on the fabrication of polymer solar cells with efficiency above 2% using an indium-free amorphous GZO-based electrode. Owen et al. suggested that polymer solar cells fabricated on GZO electrodes sputtered at a substrate temperature of 500°C have a very low PCE of 0.35%, which is much lower than that of the OSCs fabricated on GZO/Ag/GZO electrodes.[9] By further optimization of the PEDOT;PSS coating conditions and surface treatment of the GZO electrode, the performance of the OSCs fabricated on the GZO/Ag/GZO multilayer electrode might be improved. Although the GZO/Ag/GZO multilayer electrode possesses expensive Ga and Ag elements, the GZO/Ag/GZO multilayer electrode could be expected to be a low cost and indium-free TCO electrode substitute for the conventional ITO electrode because the amount of Ga (3 wt % Ga_2O_3-doped ZnO) and Ag (~12 nm) elements in the GZO/Ag/GZO multilayer is fairly small.

In summary, we propose an indium-free and low cost GZO/Ag/GZO multilayer electrode grown by dual-target sputtering at room temperature as a viable alternative to ITO electrodes for the low cost production of OSCs or flexible OSCs. By making use of the low resistivity and antireflection effect of the inserted 12 nm thick Ag layer, we obtained a GZO/Ag/GZO electrode with a very low sheet resistance of 6 Ω/□ and a high transmittance of 87%, although all of the layers were fabricated at room temperature, unlike those in a crystalline ITO electrode. The J-V performance of the OSCs fabricated on the indium-free GZO/Ag/GZO electrode indicates that the GZO/Ag/GZO electrode is a promising low cost and room-temperature-processed TCO electrode that can be used as a substitute for the high cost ITO electrode in OSCs and flexible OSCs.

This work was supported by a Korea Research Foundation grant funded by the Korean government (MOEHRD, Basic Research Promotion Fund) (no. KRF-2008-521-D00211).

Kyung Hee University assisted in meeting the publication costs of this article.

References

1. C. Brabec, V. Dyakonov, and U. Scherf, *Organic Photovoltaics*, 1st ed., Wiley-VCH Verlag, Weinheim (2008).
2. H. Spanggaard and F. C. Krebs, *Sol. Energy Mater. Sol. Cells*, **83**, 125 (2004).
3. H.-K. Kim, J.-A. Jeong, K.-H. Choi, S.-W. Jeong, and J.-W. Kang, *Electrochem. Solid-State Lett.*, **12**, H169 (2009).
4. K. Schulze, B. Maenning, K. Leo, Y. Tomita, C. May, J. Hupkes, E. Brier, E. Reinold, and P. Bauerle, *Appl. Phys. Lett.*, **91**, 073521 (2007).
5. J. van de Lagemaat, T. M. Barnes, G. Rumbles, S. E. Shaheen, T. J. Coutts, C. Weeks, I. Levitsky, J. Peltola, and P. Glatkowski, *Appl. Phys. Lett.*, **88**, 233503 (2006).
6. S.-I. Na, S.-S. Kim, J. Jo, and D.-Y. Kim, *Adv. Mater. (Weinheim, Ger.)*, **20**, 4061 (2008).
7. J. J. Berry, D. S. Ginley, and P. E. Burrows, *Appl. Phys. Lett.*, **92**, 193304 (2008).
8. V. Bhosle, J. T. Prater, F. Yang, D. Burk, and S. R. Forrest, *J. Appl. Phys.*, **102**, 023501 (2007).
9. J. Owen, M. S. Son, K.-H. Yoo, B. D. Ahn, and S. Y. Lee, *Appl. Phys. Lett.*, **90**, 033512 (2007).
10. V. Bhosle, A. Tiwari, and J. Narayan, *Appl. Phys. Lett.*, **88**, 032106 (2006).
11. J. C. Fan, F. J. Bachner, G. H. Foley, and P. M. Zavracky, *Appl. Phys. Lett.*, **25**, 693 (1974).
12. G. Haacke, *J. Appl. Phys.*, **47**, 4086 (1976).
13. D. R. Lide, *CRC Handbook of Chemistry and Physics*, 76th ed., CRC Press, Boca Raton, FL (1995).

Downloaded 25 Apr 2010 to 159.226.100.225. Redistribution subject to ECS license or copyright; see http://www.ecsdl.org/terms_use.jsp